*ANZIAM J.* 53(2012), 171–189
doi:10.1017/S1446181112000119

# CONFORMAL SLIT MAPS IN APPLIED MATHEMATICS

DARREN CROWDY[1]

(Received 7 May, 2012; revised 4 June, 2012)

**Abstract**

Conformal slit maps play a fundamental theoretical role in analytic function theory and potential theory. A lesser-known fact is that they also have a key role to play in applied mathematics. This review article discusses several canonical conformal slit maps for multiply connected domains and gives explicit formulae for them in terms of a classical special function known as the Schottky–Klein prime function associated with a circular preimage domain. It is shown, by a series of examples, that these slit mapping functions can be used as basic building blocks to construct more complicated functions relevant to a variety of applied mathematical problems.

2010 *Mathematics subject classification*: primary 30C20; secondary 31A15.

*Keywords and phrases*: conformal slit maps, Schottky–Klein prime function, multiply connected.

## 1. Introduction

The theoretical importance of conformal slit maps in the analysis of a single complex variable is well known [2, 22, 31]. Schiffer [31], for example, has elucidated a number of useful connections between conformal slit maps and the fundamental objects of potential theory such as Green's functions, modified Green's functions and harmonic measures. For applied mathematicians, especially those with a background in theoretical mechanics, what often comes to mind when conformal slit maps are mentioned is the function

$$z = \frac{1}{2}\left(\frac{1}{\zeta} + \zeta\right). \tag{1.1}$$

This is the well-known *Joukowski map* [33]. It transplants the interior of the unit disc in a complex $\zeta$-plane to the unbounded region exterior to a slit occupying the interval

[1]Department of Mathematics, Imperial College London, 180 Queen's Gate, London SW7 2AZ, UK; e-mail: d.crowdy@imperial.ac.uk.

$[-1, 1]$ along the real axis in a complex $z$-plane. In applications, this slit might model a flat plate, an aerofoil, a defect or dislocation in an elastic medium, or a gap in a wall.

But suppose the problem at hand involves *two* slits (that is, two aerofoils, defects, or gaps in the wall). What is the generalization of the Joukowski map then? It is possible to find formulae for such maps, expressed in terms of elliptic functions, in classical texts on conformal mapping such as the monograph by Nehari [27] (see also the book by Sedov [33]). But such explicit formulae for maps to doubly connected domains are rare. Moreover, if a problem involves *three* or more slits, elliptic function theory is no longer relevant (in general) and the standard literature is then virtually devoid of any analytical results. In practice it is common to defer, in such cases, to purely numerical methods.

The message of this review article is that a constructive analytical theory exists for multiply connected conformal slit maps and that the latter find abundant use in applications. This theory has been developed by the author and his collaborators in recent years, and it relies on the use of a classical special function, hardly known to nonspecialists, called the *Schottky–Klein prime function* [1]. For a taste of its usefulness, the reader is invited to verify directly that the Joukowski map (1.1) can be rewritten in the form

$$z = \frac{\omega^2(\zeta, -1) + \omega^2(\zeta, 1)}{\omega^2(\zeta, -1) - \omega^2(\zeta, 1)} \tag{1.2}$$

if we define

$$\omega(\zeta, \alpha) = (\zeta - \alpha). \tag{1.3}$$

This apparently innocuous rewriting of the Joukowski map has particular significance once it is recognized that the function (1.3) is just one manifestation (indeed the simplest one) of a Schottky–Klein prime function.

A circular domain is a domain whose boundaries are all circles. On the left in Figure 1, two other circular domains besides the simple unit disc are shown: the concentric annulus domain is doubly connected, and the domain comprising the unit disc with two excised interior circular discs is triply connected. These circular domains can be conformally mapped to the *multiple* slit domains shown to the right of each in Figure 1 by the very same map (1.2). The only difference is that the definition of $\omega(\cdot, \cdot)$ changes in each case: it must be chosen to be the Schottky–Klein prime function associated with that particular circular domain. In Figure 1 each circular boundary $C_j$ maps to the slit $S_j$ on the real axis in the image domain.

This simple illustration points to the more general fact that, in many instances, reinterpreting well-known results—in this case, the Joukowski map (1.1)—in terms of the Schottky–Klein prime function can give important clues to useful generalizations. In this respect, formula (1.2) might be viewed as a generalized Joukowski map to *any* number of slits on the real axis.

https://doi.org/10.1017/S1446181112000119 Published online by Cambridge University Press

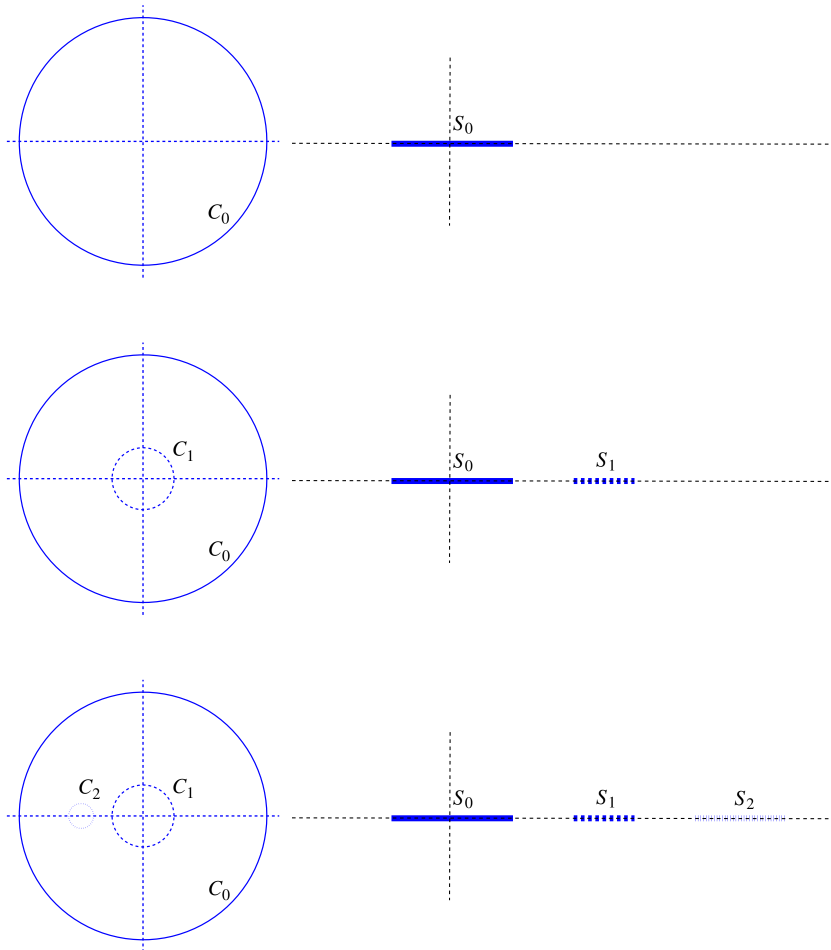


FIGURE 1. Each circular domain on the left is transplanted to the slit domain on the right by the map (1.2). The only difference in each case is the definition of the Schottky–Klein prime function $\omega(\cdot, \cdot)$.

## 2. The simplest prime function

The Schottky–Klein prime function is a classical mathematical object discussed, for example, in Baker's 19th-century monograph on abelian functions [1], but it is not well known. Every mathematician has, however, come across the simplest instance of it. The fundamental theorem of algebra states that any $N$th-degree polynomial $P_N(\zeta)$, with $N \geq 1$, can be uniquely factorized into a product of simpler functions in the form

$$P_N(\zeta) = \zeta^N + a_{N-1}\zeta^{N-1} + \cdots + a_1\zeta + a_0 = \prod_{k=1}^{N}(\zeta - \gamma_k),$$

where $\{\gamma_k \mid k = 1, \ldots, N\}$ are the roots of the polynomial. It is natural to define the simple monomial function of two variables $\omega(\zeta, \gamma) = (\zeta - \gamma)$ to be a *prime function* because, by analogy with the fact that any integer can be factorized into a unique product of prime integers, any polynomial can be uniquely factorized into a product of such prime functions, namely,

$$P_N(\zeta) = \prod_{k=1}^{N} \omega(\zeta, \gamma_k).$$

By extension, any rational function $R(\zeta)$ (a function whose only singularities in the extended complex plane, or Riemann sphere, are poles) can be written in the form

$$R(\zeta) = \frac{\prod_{k=1}^{N} \omega(\zeta, \alpha_k)}{\prod_{k=1}^{N} \omega(\zeta, \beta_k)}, \tag{2.1}$$

where $\{\alpha_k \mid k = 1, \ldots, N\}$ are the zeros and $\{\beta_k \mid k = 1, \ldots, N\}$ the poles of the function. The Schottky–Klein (SK) prime function is the name given to the function that replaces the simple monomial function $(\zeta - \gamma)$ when the underlying compact Riemann surface has higher genus than the Riemann sphere. Any meromorphic function $R(\zeta)$ on such a surface then also has a representation in terms of its zeros and poles that is very much akin to (2.1). The prime function for general compact Riemann surfaces was first considered by Klein [25] and Schottky [32]. It is discussed by Burnside [3] and treated in a special chapter of the classic monograph by Baker [1]. It has close mathematical connections with the notion of a *prime form* [21] on the Jacobi variety associated with a compact Riemann surface, and prime forms have, over the years, found much application in, for example, algebraic geometry, mathematical physics and integrable systems theory.

The SK prime function within the Schottky model of algebraic curves has, by contrast, been used much less often, and, in particular, its relevance to analysis in multiply connected domains has only very recently been formulated and explored, principally by the author and his group. Hejhal [24] considers the SK prime function in his discussion of the classical kernel functions of planar domains, and it is on the particular application of the prime function to planar domains that the present article focuses. It is possible to associate with any multiply connected planar domain a compact symmetric Riemann surface called its Schottky double [23]. The SK prime function on such symmetric Riemann surfaces has certain special properties which are reviewed here. Consequently, a large number of results associated with the function theory of planar domains can be conveniently expressed in terms of the SK prime function on the Schottky double of the domain.

## 3. A more complicated prime function

The SK prime function for the Riemann sphere is simple and familiar; the prime function for a sphere with one handle, or the torus, is more interesting. One

https://doi.org/10.1017/S1446181112000119 Published online by Cambridge University Press

mathematical model of a torus is to consider the two neighbouring annuli $\rho < |\zeta| < 1$ and $1 < |\zeta| < 1/\rho$, where $0 < \rho < 1$ is a real parameter. These two annuli will constitute the two symmetric "sides" of the Schottky double. They already meet at the circle $|\zeta| = 1$ but we also want them to be associated at the two other boundary circles $|\zeta| = \rho$ and $|\zeta| = 1/\rho$. A holomorphic identification of these two circles is provided by the Möbius map $\zeta \mapsto \rho^2\zeta$. A meromorphic function $F(\zeta)$ on this torus can be defined as a function satisfying the functional relation

$$F(\rho^2\zeta) = F(\zeta) \tag{3.1}$$

and having only poles in the annulus $\rho \leq |\zeta| < \rho^{-1}$. By the functional relation (3.1), $F(\zeta)$ will have poles in all other so-called *equivalent annuli* obtained by repeatedly mapping the annulus $\rho \leq |\zeta| < \rho^{-1}$ under the transformation $\zeta \mapsto \rho^2\zeta$, or its inverse $\zeta \mapsto \rho^{-2}\zeta$ (these will produce a tessellation of the plane). Meromorphic functions satisfying (3.1) have been dubbed *loxodromic functions* [35].

But how do we construct functions satisfying (3.1)? Consider the function $P(\zeta)$ defined by the infinite product

$$P(\zeta) = (1 - \zeta) \prod_{k=1}^{\infty} (1 - \rho^{2k}\zeta)(1 - \rho^{2k}\zeta^{-1}). \tag{3.2}$$

(Notice that this function depends on the parameter $\rho$, but our notation does not include this parameter explicitly as an argument of the function.) Using standard methods for infinite products [35], the function (3.2) can be shown to be absolutely convergent for all $\zeta \neq 0$ and $0 < \rho < 1$. It is easy to confirm, directly from this definition, that $P(\zeta)$ satisfies the functional relation

$$P(\rho^2\zeta) = -\zeta^{-1}P(\zeta). \tag{3.3}$$

The function $P(\zeta)$ does not itself satisfy (3.1), but the ratio of products

$$R(\zeta) = \frac{\prod_{k=1}^{N} P(\zeta\alpha_k^{-1})}{\prod_{k=1}^{N} P(\zeta\beta_k^{-1})} \tag{3.4}$$

*does* satisfy (3.1) provided the parameters $\{\alpha_k, \beta_k \mid k = 1, \ldots, N\}$, which are all points inside the annulus $\rho < |\zeta| < \rho^{-1}$, satisfy the single condition

$$\prod_{k=1}^{N} \alpha_k = \prod_{k=1}^{N} \beta_k.$$

This result is a simple exercise based on use of (3.3). By inspection, $R(\zeta)$ can be seen to have only poles in the annulus $\rho \leq |\zeta| < \rho^{-1}$, and is therefore meromorphic on the torus. On comparing (3.4) with (2.1) it is natural to identify the function $P(\zeta)$ with the prime function for the torus, and, up to normalization by a multiplicative constant, this is indeed the case.

An important observation is that since $P(\zeta)$ is analytic in the annulus $\rho < |\zeta| < 1$, in addition to the infinite product expression (3.2) it also has a convergent Laurent series there. By making use of (3.3), this can be shown to be given by the rapidly convergent series

$$P(\zeta) = A \sum_{n=-\infty}^{\infty} (-1)^n \rho^{n(n-1)} \zeta^n, \tag{3.5}$$

where

$$A = \frac{\prod_{n=1}^{\infty}(1+\rho^{2n})^2}{\sum_{n=1}^{\infty} \rho^{n(n-1)}}.$$

The Laurent series (3.5) converges everywhere in the annulus $\rho \le |\zeta| < \rho^{-1}$. These two representations of the same function furnish the identity

$$(1-\zeta)\prod_{k=1}^{\infty}(1-\rho^{2k}\zeta)(1-\rho^{2k}\zeta^{-1}) = A \sum_{n=-\infty}^{\infty} (-1)^n \rho^{n(n-1)} \zeta^n, \tag{3.6}$$

which relates an infinite product to an infinite sum. The relation (3.6) is known as the *Jacobi triple product identity* [36].

## 4. The Schottky–Klein prime function

The Riemann mapping theorem, which says that any simply connected domain is conformally equivalent to the unit disc, has been generalized by Koebe (see, for example, the monograph by Goluzin [22]) to the case of planar domains of finite connectivity. Any multiply connected planar domain of connectivity $M+1$ is known to be conformally equivalent to a canonical *circular domain* $D_\zeta$ of the following form. Consider the unit $\zeta$-disc in a complex $\zeta$-plane and excise $M$ smaller circular discs centred at points $\{\delta_j \in \mathbb{C} \mid j = 1, \ldots, M\}$ and having radii $\{q_j \in \mathbb{R} \mid j = 1, \ldots, M\}$. The unit circle is denoted by $C_0$ and the boundary circles of the interior discs by $\{C_j \mid j = 1, \ldots, M\}$. The resulting domain $D_\zeta$ is a circular domain of connectivity $M+1$; the data $\{\delta_j, q_j \mid j = 1, \ldots, M\}$ are the *conformal moduli* of the domain.

Given any such circular domain $D_\zeta$, there exists a special transcendental function associated with it: the SK prime function [1], denoted by $\omega(\zeta, \alpha)$. It is ostensibly a function of two variables $\zeta$ and $\alpha$, but it also depends on the geometrical data $\{q_k, \delta_k \mid k = 1, \ldots, M\}$ characterizing the domain $D_\zeta$ (but, again, our notation does not include these explicitly as arguments of the function).

There are two known ways to evaluate the SK prime function. There is a classical infinite product for it that is described by Baker [1]; in the case $M = 1$, the product (3.2) is precisely such a representation. Alternatively, Crowdy and Marshall [16] have devised a novel numerical method for calculating $\omega(\cdot,\cdot)$ based on representations of it in terms of Fourier–Laurent series. The motivating idea behind the latter numerical method is to extend the Jacobi triple product identity (3.6) (relevant only for $M = 1$) to the general multiply connected case. Downloadable MATLAB files for the

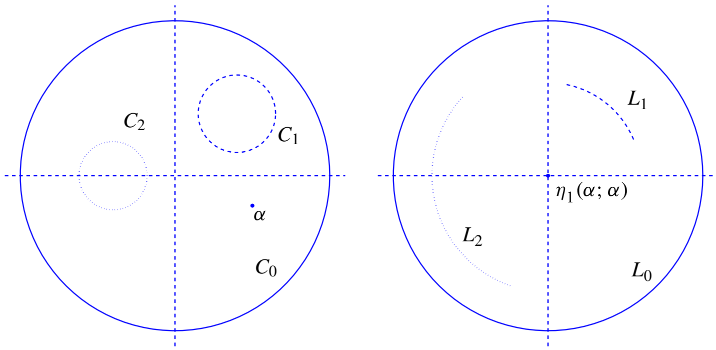


FIGURE 2. A circular domain $D_\zeta$ (left) and a circular slit domain (right). The circular slit map $\eta_1(\zeta;\alpha)$ in (5.1) maps $D_\zeta$ to the circular slit domain, with $C_0$ mapping to the unit circle $L_0$, and $C_1$ and $C_2$ mapping to concentric circular arc slits $L_1$ and $L_2$ inside $L_0$. The point $\alpha$ maps to the centre of the circle $L_0$. The domains shown are triply connected ($M = 2$).

computation of $\omega(\cdot,\cdot)$ based on this method are available [12]. Given these resources, for the remainder of this paper we treat the SK prime function as a readily computable special function.

## 5. Prime functions and conformal slit maps

It is a remarkable and useful fact that conformal maps of multiply connected circular domains to all the canonical slit domains [2, 27] can be expressed explicitly, as concise formulae, in terms of the SK prime function. This was first pointed out by Crowdy and Marshall [15]. Those formulae relevant to the remainder of this article are now reviewed. For full details of the properties of the prime function leading to all the results stated below, the reader should refer to the paper by Crowdy and Marshall [15].

**5.1. Circular slit domains** Pick a point $\alpha$ in the interior of some multiply connected circular domain $D_\zeta$ as shown in Figure 2 for the case $M = 2$. Consider the function

$$\eta_1(\zeta;\alpha) = \frac{\omega(\zeta,\alpha)}{|\alpha|\omega(\zeta,\overline{\alpha}^{-1})}. \tag{5.1}$$

As a conformal map this takes $C_0$ to a unit circle $L_0$ and the point $\zeta = \alpha$ to the centre of $L_0$; the circles $C_1$ and $C_2$ are mapped to circular arc slits $L_1$ and $L_2$ concentric with the circle $L_0$. The image domain is a circular slit domain recognized as being one of the canonical multiply connected slit domains [2, 27].

**5.2. Half-space slit domains** Consider the function

$$\eta_2(\zeta;\alpha_1,\alpha_2) = \frac{\omega(\zeta,\alpha_1)}{\omega(\zeta,\alpha_2)},$$

where the two parameters $\alpha_1$ and $\alpha_2$ are both taken to be on the same boundary circle of a multiply connected circular domain $D_\zeta$. Figure 3 shows the case with $M = 2$,

https://doi.org/10.1017/S1446181112000119 Published online by Cambridge University Press

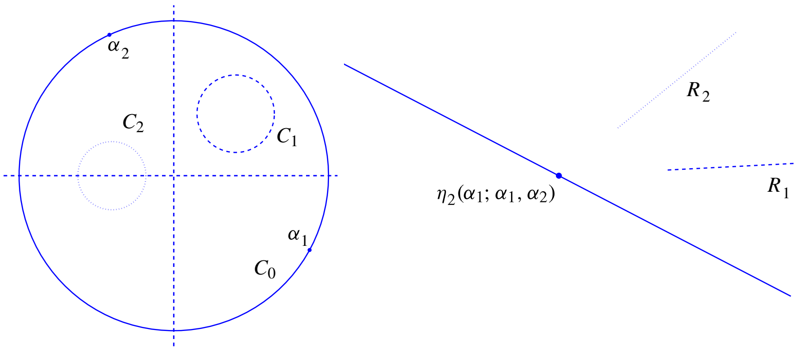


FIGURE 3. A half-space slit domain (right) and the preimage circular domain $D_\zeta$ (left). Under the map $\eta_2(\zeta; \alpha_1, \alpha_2)$, $C_0$ maps to an infinite straight line through the origin and infinity while $C_1$ and $C_2$ map to radial slits $R_1$ and $R_2$. The point $\alpha_1$ maps to the origin and the point $\alpha_2$ maps to infinity.

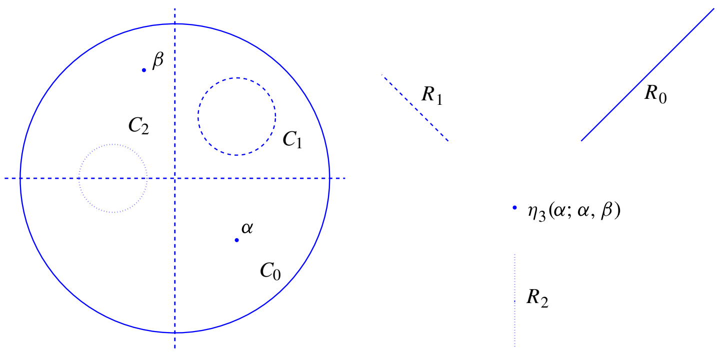


FIGURE 4. A radial slit domain (right) and the preimage circular domain $D_\zeta$ (left). Under the map $\eta_3(\zeta; \alpha, \beta)$, the circles $\{C_j \mid j = 0, 1, 2\}$ map to radial slits $\{R_j \mid j = 0, 1, 2\}$ of finite length. The point $\alpha$ maps to the origin and the point $\beta$ maps to infinity.

with $\alpha_1$ and $\alpha_2$ both chosen to be on $C_0$. The point $\alpha_1$ maps to the origin and the point $\alpha_2$ maps to infinity in such a way that $C_0$ maps to an infinite straight line through the origin. The circles $C_1$ and $C_2$ are each transplanted to radial slits of finite length. This image domain is referred to as a half-space slit domain. Actually, such domains are not discussed explicitly by Crowdy and Marshall [15], but they are a special case of the radial slit maps presented next.

**5.3. Radial slit domains** Pick two points $\alpha$ and $\beta$ strictly inside a multiply connected circular domain $D_\zeta$ and consider the function

$$\eta_3(\zeta; \alpha, \beta) = \frac{\omega(\zeta, \alpha)\omega(\zeta, \overline{\alpha}^{-1})}{\omega(\zeta, \beta)\omega(\zeta, \overline{\beta}^{-1})}.$$

As a conformal map this takes $\zeta = \alpha$ to the origin and $\zeta = \beta$ to infinity. It also maps all the circles $\{C_j \mid j = 0, 1, \ldots, M\}$ to radial slits $\{R_j \mid j = 0, 1, \ldots, M\}$ which are

https://doi.org/10.1017/S1446181112000119 Published online by Cambridge University Press

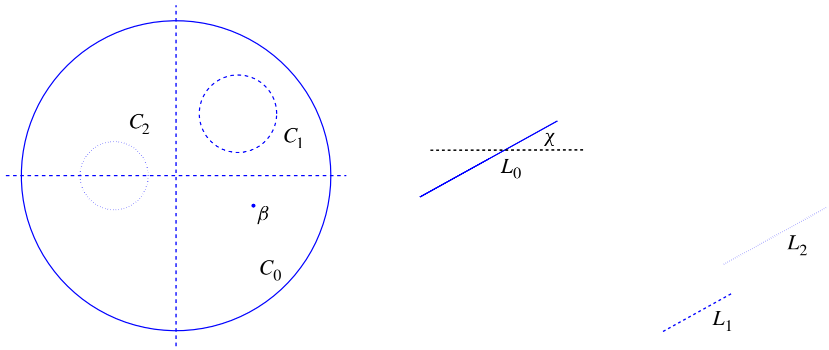


FIGURE 5. A parallel slit domain (right) and the preimage circular domain $D_\zeta$ (left). Under the map $\eta_4(\zeta;\chi)$, the circles $\{C_j \mid j = 0, 1, 2\}$ map to parallel slits $\{L_j \mid j = 0, 1, 2\}$ each making an angle $\chi$ to the real axis. The point $\beta$ maps to infinity.

finite-length intervals on rays emanating from the origin. Figure 4 shows a schematic in a triply connected case.

**5.4. Parallel slit domains** Consider the function

$$\eta_4(\zeta;\chi) = a\left[\left\{\frac{\partial}{\partial\alpha} - e^{2i\chi}\frac{\partial}{\partial\overline{\alpha}}\right\}\log\eta_1(\zeta;\alpha)\right]_{\alpha=\beta} + b,$$

where $a, \chi \in \mathbb{R}$ and $b \in \mathbb{C}$ are constants. This maps the circular domain $D_\zeta$ to the unbounded domain exterior to $M + 1$ parallel slits each making angle $\chi$ to the positive real axis and with the point $\zeta = \beta$ mapping to infinity. Figure 5 shows a schematic in which the circles $\{C_j \mid j = 0, 1, 2\}$ map to parallel slits $\{L_j \mid j = 0, 1, 2\}$.

## 6. Conformal slit maps in applications

The remaining sections of this paper survey a series of example applications where the conformal slit maps mentioned above play a useful role in providing solutions to various problems. The aim is to demonstrate the versatility of the methods and to alert the reader to the potential of the ideas. In each problem, the reader will see that the conformal slit maps discussed above play a central role in building expressions for the solutions.

**6.1. Point vortices and sources in ideal flow** As a first example, consider two-dimensional, ideal, irrotational fluid flow in some unbounded region $D$ exterior to $M + 1$ solid objects with impenetrable boundaries, with $M \geq 0$. The objects might be aerofoils, islands or obstacles, depending on the application. To fix ideas, Figure 6 shows a schematic of a geophysical flow in which there are three islands off a coastline with an outlet into the ocean, perhaps from a river basin entering the sea. The fluid in this case is quadruply connected, so that $M = 3$. In a simple model, the flow from a river outlet might be modelled as a so-called *point source* singularity, and the oceanic eddies moving around the islands might be modelled as *point vortices*.

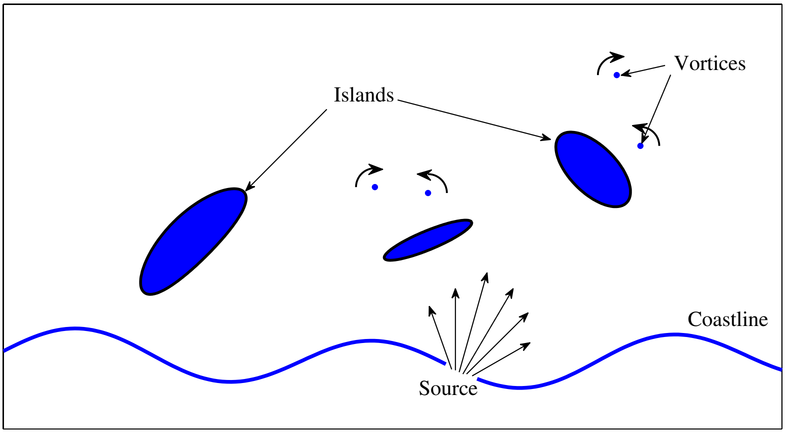


FIGURE 6. Schematic of an ideal flow in a multiply connected situation. The flow from a river outlet, say, in a coastline might be modelled as a point source; the oceanic eddies moving around the islands can be modelled as point vortices.

To elucidate these singularity models, let $w(z)$ be the (instantaneous) complex potential for the flow. This is the complex analytic function of the variable $z = x + iy$ such that the two-dimensional velocity field $(u, v)$ is given by

$$u - iv = \frac{dw}{dz}.$$

A point *source* of strength $m$ at $z_\alpha$ is defined to be a logarithmic singularity with the local form near $z = z_\alpha$ given by

$$w(z) = \frac{m}{2\pi} \log(z - z_\alpha) + \text{locally analytic function}. \tag{6.1}$$

A *point vortex* at $z_\alpha$ of circulation $\Gamma$ corresponds to a singularity of $w(z)$ having local form near $z = z_\alpha$ given by

$$w(z) = -\frac{i\Gamma}{2\pi} \log(z - z_\alpha) + \text{locally analytic function}. \tag{6.2}$$

While (6.1) and (6.2) differ only in whether the strength of the logarithmic singularity is purely real or purely imaginary, the functional forms of the associated complex potentials are rather different and involve distinct types of conformal slit map. More background on the basic singularities of two-dimensional ideal fluid flows can be found in standard fluid dynamics texts [26, 33].

Let $D_\zeta$ denote a circular domain that is conformally equivalent to $D$ and let $z(\zeta)$ be the conformal mapping from $D_\zeta$ to $D$. There is a (hopefully harmless) abuse of notation here in that the symbol $z$ is used to denote both the coordinate in the image domain and the function that carries out the mapping to that domain. A point $\beta$ maps

https://doi.org/10.1017/S1446181112000119 Published online by Cambridge University Press

to infinity so that, near $\zeta = \beta$,

$$z(\zeta) = \frac{a}{\zeta - \beta} + \text{locally analytic function}$$

for some constant $a$. Let $z_\alpha = z(\alpha)$ so that $\alpha$ is the preimage in $D_\zeta$ of $z_\alpha$. Define

$$W(\zeta) = w(z(\zeta)).$$

In order to satisfy the condition that the boundaries of $D$ are streamlines, the conformal invariance of the boundary value problem implies that $W(\zeta)$ has constant imaginary part on the boundaries of $D_\zeta$. Moreover, a local analysis shows that, for a point source or a point vortex, $W(\zeta)$ inherits the same logarithmic singularity as $w(z)$. So for a point source of strength $m$,

$$W(\zeta) = \frac{m}{2\pi} \log(\zeta - \alpha) + \text{locally analytic function,}$$

and for a point vortex of circulation $\Gamma$,

$$W(\zeta) = -\frac{i\Gamma}{2\pi} \log(\zeta - \alpha) + \text{locally analytic function.}$$

The complex potential $W(\zeta)$ for a point source of strength $m$ at a point $z_\alpha$ can be built using conformal slit maps. It is

$$W(\zeta) = \frac{m}{2\pi} \log[\eta_3(\zeta; \alpha, \beta)], \tag{6.3}$$

where $\eta_3(\zeta; \alpha, \beta)$ is the radial slit map of Section 5.3. The complex potential (6.3) has the required logarithmic singularity at $\alpha$ and has constant imaginary part on all the boundaries of $D_\zeta$; its imaginary part on $C_j$ is the value of $[m/(2\pi)]\arg[\eta_3(\zeta; \alpha, \beta)]$ on $C_j$, which is constant because $\eta_3(\zeta; \alpha, \beta)$ is a radial slit map having constant argument on $C_j$ for $j = 0, 1, \ldots, M$. The function (6.3) also has a sink at $\beta$, corresponding to a far-field sink in the physical domain $D$, as required by conservation of mass. To uniquely define a two-dimensional ideal flow taking place in the unbounded region exterior to a set of objects, it is necessary to specify the circulation around each of those objects. It can be shown that (6.3) gives a zero circulation around each object.

On the other hand, the complex potential for a point vortex of circulation $\Gamma$ at the point $z_\alpha$ in the same domain is

$$W(\zeta) = -\frac{i\Gamma}{2\pi} \log\left[\frac{\eta_1(\zeta; \alpha)}{\eta_1(\zeta; \beta)}\right], \tag{6.4}$$

where $\eta_1(\zeta; \alpha)$ is the circular slit map of Section 5.1. This function has the effect of putting a point vortex of opposite circulation at infinity in order that the circulations around all the obstacles are zero. More details of point vortex and source/sink flows in multiply connected domains are given by Crowdy and Marshall [4, 8, 14].

Formulae (6.3) and (6.4) reflect the central role played by the canonical conformal slit maps in this classical application. It is interesting to point out, however, that neither (6.3) nor (6.4) can be found in standard fluid dynamics texts, except in the simply connected case. More generally, it turns out that the ideas outlined above can be extended to devise a new and very general "calculus" for analysing two-dimensional ideal flows in multiply connected domains [8].

**6.2. Hele-Shaw flows** Hele-Shaw flows, or Laplacian growth problems, constitute a paradigmatic free boundary problem arising, in various guises, in many different physical applications. For flow of viscous fluid between the two plates of a Hele-Shaw cell, the pressure satisfies the two-dimensional Laplace equation, and so complex variable methods are again available. An important basic problem dates back to Taylor and Saffman [34], who studied the situation where a single bubble of less viscous fluid, such as air, travels steadily along a channel in a Hele-Shaw cell containing a much more viscous fluid, such as oil. The bubble is assumed to be at constant pressure with no surface tension on its boundary. The free boundary problem is to ascertain the shape, and speed, of this bubble as it travels steadily along the channel. Taylor and Saffman [34] also assumed that the bubble is symmetric across the channel centreline so that they could take advantage of the classical Schwarz–Christoffel formula [20] to find their solution. (The general topic of Schwarz–Christoffel maps is discussed again in Section 6.5.)

One generalization of the Taylor–Saffman problem is the *multiple* bubble problem, that is, to consider $M + 1$ constant-pressure bubbles, for $M > 0$, co-travelling in a steady arrangement in free space (with no channel walls) and to ask about their shapes as they travel. Figure 7 shows a schematic of this arrangement when $M = 2$. An averaging of the Navier–Stokes equations over the thin layer of fluid between the two plates of a Hele-Shaw cell implies that the pressure field exterior to the bubbles is harmonic, and that it is proportional to a velocity potential $\phi$, so that the fluid velocity $\mathbf{u} = \nabla\phi$.

This free boundary problem can also be solved using the conformal slit maps introduced earlier. It is natural to move to a co-travelling frame of reference in which the bubble configuration is steady. Suppose the bubbles all travel at speed $U$ in a background uniform flow with unit speed $V = 1$. The mathematical problem then reduces to finding the complex potential $w(z) = \phi + i\psi$ for the flow (where $\psi$ is a streamfunction), as well as the conformal map $z(\zeta)$ from a canonical circular preimage region to the flow domain; the latter will give information on the bubble shapes. Since the flow exterior to the bubbles is unbounded, we require

$$z(\zeta) \sim \frac{a}{\zeta - \beta} + \text{locally analytic function} \tag{6.5}$$

near some point $\beta$ in $D_\zeta$ which maps to infinity. As in the previous problem, it is expedient to introduce

$$W(\zeta) = w(z(\zeta)).$$

https://doi.org/10.1017/S1446181112000119 Published online by Cambridge University Press

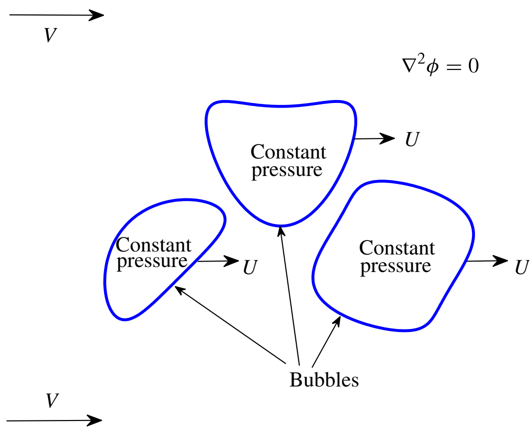


FIGURE 7. Three constant-pressure bubbles in an unbounded Hele-Shaw cell co-travelling steadily with speed $U$ in a uniform flow $V$. The free boundary problem is to find the equilibrium bubble shapes. The velocity potential $\phi$ is harmonic exterior to the bubbles.

On the boundaries of all the co-travelling bubbles, which must be streamlines, we require

$$\psi = \mathrm{Im}[W(\zeta)] = \text{constant} \tag{6.6}$$

with $W(\zeta)$ having the local behaviour

$$W(\zeta) \sim (1 - U)z \sim \frac{(1 - U)a}{\zeta - \beta} \tag{6.7}$$

as $\zeta \to \beta$. The condition that the fluid pressure is constant on all bubble boundaries reduces to the condition that

$$\mathrm{Re}[S(\zeta)] = \text{constant} \quad \text{where } S(\zeta) = W(\zeta) + Uz(\zeta). \tag{6.8}$$

It is clear from (6.5) and (6.7) that, as $\zeta \to \beta$,

$$S(\zeta) \sim \frac{a}{\zeta - \beta}. \tag{6.9}$$

Once $W(\zeta)$ and $S(\zeta)$ have been found, the conformal map $z(\zeta)$ can be determined and, hence, so can the shape of the steadily translating bubbles.

Inspection of (6.6) and (6.7) shows that $W(\zeta)$ shares the same properties as a conformal map from $D_\zeta$ to an unbounded parallel slit region with slits all parallel to the real axis. On the other hand, from (6.8) and (6.9), $S(\zeta)$ is seen to share the properties of a conformal map from $D_\zeta$ to an unbounded parallel slit region with slits all parallel to the imaginary axis. The required solution therefore turns out to have the form

$$W(\zeta) = c_1\eta_4(\zeta; 0), \qquad S(\zeta) = c_2\eta_4(\zeta; \pi/2),$$

https://doi.org/10.1017/S1446181112000119 Published online by Cambridge University Press

where $c_1$ and $c_2$ are constants chosen to ensure that the appropriate far-field conditions (6.7) and (6.9) are satisfied and $\eta_4(\zeta;\chi)$ is the parallel slit map of Section 5.4. With $W(\zeta)$ and $S(\zeta)$ determined, the conformal map $z(\zeta)$ can be found. We refer the reader to an earlier paper by the author [7] for more details but, once again, the role of the conformal slit maps is clear.

**6.3. Hollow vortices** A hollow vortex is a finite-area, constant-pressure region $D$ having a nonzero circulation around it [30]. Let its boundary be denoted by $\partial D$. It is usually supposed that the fluid, of density $\rho$, exterior to the hollow vortex is irrotational and, hence, described mathematically by a complex potential $w(z)$ whose imaginary part is the streamfunction for the flow. The derivative of $w(z)$ with respect to $z$ gives the velocity components $\mathbf{u} = (u, v)$ in the complex form

$$\frac{dw}{dz} = u - iv.$$

In a steady configuration the boundary of the hollow vortex is a streamline, so that

$$\mathrm{Im}[w(z)] = \text{constant} \quad \text{on } \partial D. \tag{6.10}$$

Bernoulli's theorem [26] provides the fluid pressure $p$ from the relation

$$\frac{p}{\rho} + \frac{1}{2}\left|\frac{dw}{dz}\right|^2 = \text{constant},$$

and, in order that the fluid pressure on the vortex boundary be continuous with the constant internal pressure, it is therefore necessary that

$$\left|\frac{dw}{dz}\right| = \text{constant} \quad \text{on } \partial D. \tag{6.11}$$

Recently, several new analytical solutions for hollow vortex equilibria have been discovered by using free streamline theory combined with the conformal slit maps discussed here. To give an idea of the solution method, consider the two functions

$$W(\zeta) = w(z(\zeta)), \qquad R(\zeta) = \frac{dw}{dz}.$$

The boundary condition (6.10) suggests that $W(\zeta)$ is related to a parallel slit map of Section 5.4, with angle $\chi = 0$, while (6.11) suggests that $R(\zeta)$ is related to the circular slit map of Section 5.1. This is indeed the case, and expressions for $W(\zeta)$ and $R(\zeta)$ can be determined explicitly. The chain rule then provides the functional form of the relevant conformal map $z(\zeta)$, and hence the shape of the vortices, via the relations

$$R(\zeta) = \frac{dw}{dz} = \frac{dW/d\zeta}{dz/d\zeta} \quad \text{or} \quad \frac{dz}{d\zeta} = \frac{dW/d\zeta}{R(\zeta)}.$$

Using these ideas, the doubly connected SK prime function of Section 3 has recently been used to find a new class of exact solutions for a von Kármán vortex street comprising two rows of hollow vortices [13]. A superposition of such streets of hollow vortices with gradually increasing areas is illustrated in Figure 8.

https://doi.org/10.1017/S1446181112000119 Published online by Cambridge University Press

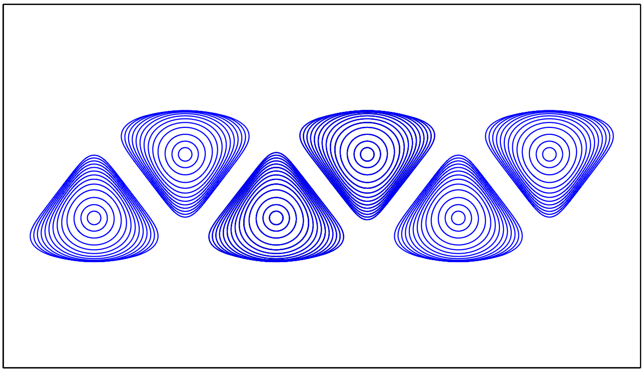


FIGURE 8. Superposition of staggered von Kármán streets of hollow vortices with gradually increasing areas. Three periods of each singly periodic array of vortices are shown. All solutions travel in the horizontal direction at speed $U = 0.4$.

**6.4. Superhydrophobic surfaces** The use of conformal slit maps in applications is not restricted just to flows involving Laplace's equation. They can also be used to solve problems involving low Reynolds number flows which, in two dimensions, are governed by a biharmonic equation for the streamfunction $\psi$, that is,

$$\nabla^4 \psi = 0.$$

There has been much recent interest, owing to technological advances and applications in microfluidics, in so-called superhydrophobic surfaces and the quantification of their "effective slip lengths". This is a measure of the frictional properties of the surface: it is the fictional distance below the surface at which the velocity profile of a low-Reynolds number shear flow over it would extrapolate to zero [29].

For shear flows with shear rate $\dot{\gamma}$ over such a surface occupying the plane $y = 0$, the velocity field far from the plane of the surface, as $y \to \infty$, takes the form

$$\mathbf{u} = (\dot{\gamma} y + \dot{\gamma} \lambda)\hat{\mathbf{x}},$$

where $\hat{\mathbf{x}}$ is the flow direction. Figure 9 shows a schematic of a surface at $y = 0$ with a shear flow over it making angle $\phi$ with the positive $x$-direction. The constant $\lambda$ is the *effective slip length*. Larger slip lengths correspond to reduced frictional properties. The slip length also depends on the direction $\phi$ of the shear flow. If the flow is parallel to the length of the grooves, so that $\phi = \pi/2$ in the schematic of Figure 9, the slip length has the value $\lambda^{\parallel}$; if the flow is perpendicular to the length of the grooves, so that $\phi = 0$ in Figure 9, the associated slip length is denoted by $\lambda^{\perp}$. To find $\lambda^{\parallel}$ and $\lambda^{\perp}$ it is necessary to solve two distinct flow problems.

It turns out that the solution to *both* flow problems can be reduced to finding two conformal maps, $z(\zeta)$ and $H(\zeta)$, from a canonical $(M + 1)$-connected circular

https://doi.org/10.1017/S1446181112000119 Published online by Cambridge University Press

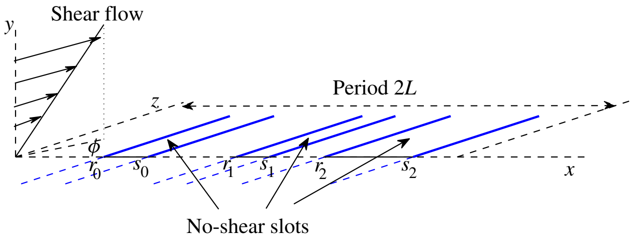


FIGURE 9. Shear flow over a surface at $y = 0$ with a $2L$-periodic array of $M + 1$ no-shear grooves, or "slots", in each period window extending along the $z$-direction. In between the slots, the surface is a no-slip surface. A single period window of the $M = 2$ case is shown. The shear flow makes angle $\phi$ to the direction of the slots. The mathematical problem is to determine the effective slip length of such a surface.

region $D_\zeta$. The first is the conformal map $z(\zeta)$ to the period strip $x \in [0, 2L]$, $-\infty < y < \infty$, with $M + 1$ horizontal slits along the real axis as shown in Figure 9 in the case $M = 2$. A second map, denoted $H(\zeta)$, is to the same period strip but now with $M + 1$ vertical slits centred on the real axis. It is found that these maps are given explicitly as

$$z(\zeta) = -\frac{iL}{\pi} \log\left[\frac{\eta_1(\zeta; \alpha)}{\eta_1(\zeta; \overline{\alpha})}\right], \quad H(\zeta) = -\frac{iL}{\pi} \log[\eta_3(\zeta; \alpha, \overline{\alpha})], \tag{6.12}$$

where $\alpha$ is a point in $D_\zeta$ and $\eta_1$ and $\eta_3$ are the conformal slit maps of Sections 5.1 and 5.3. The central role played by conformal slit maps is again clear.

Philip [28] found the solution for the slip lengths in the simplest case when $M = 0$. Philip's result can be stated as

$$\lambda^{\parallel} = \frac{c}{\pi\delta} \log(\sec(\pi\delta/2)) = 2\lambda^{\perp}, \tag{6.13}$$

where $\delta = c/(2L)$. The results (6.12) can be used to show that this is the simplest case of a more general result expressed concisely as

$$\lambda^{\parallel} = \frac{2L}{\pi} \log\left|\frac{\omega(\alpha, 1/\alpha)}{\omega(\alpha, 1/\overline{\alpha})}\right| = 2\lambda^{\perp}. \tag{6.14}$$

Philip's result (6.13) is retrieved when $M = 0$ and the prime function is simply $\omega(\zeta, \alpha) = (\zeta - \alpha)$. For more general choices of the SK prime function, (6.14) gives the longitudinal and transverse slip lengths when there are $M + 1$ no-shear slots, of arbitrary position and length, in each period window. The formula (6.14) is clearly relevant to a much more general class of superhydrophobic surfaces. More details of the derivation of (6.12) are given by the author in an earlier paper [10].

**6.5. Schwarz–Christoffel maps** The conformal slit maps of Section 5 are simple examples of maps from circular preimage domains to *polygonal* and *polycircular arc* domains. Polygonal domains have boundaries that are a union of straight-line segments; polycircular arc domains have boundaries that are a union of arcs of circles, including straight-line segments with zero curvature. It is perhaps not surprising, then, that these basic slit maps have been found [5, 6] to provide "building block functions" in constructing generalizations of the classical *Schwarz–Christoffel formula* [20] to the case of multiply connected polygonal domains. This central role played by conformal slit maps in the construction of a generalized Schwarz–Christoffel formula to multiply connected polygonal domains in terms of the SK prime function has been elucidated by the author in an earlier paper [9].

The topic of multiply connected Schwarz–Christoffel maps has been an active area of research in recent years, with several groups of workers making contributions [5, 6, 17–19]. Moreover, a new approach, based on the SK prime function, to the conformal mapping of multiply connected polycircular arc domains has been presented by Crowdy et al. [11].

## 7. Conclusion

The Schottky–Klein prime function on the Schottky double of a planar domain provides an important linchpin in the function theory associated with planar multiply connected domains. As indicated in this review, it has many applications in this area and it is only recently that many of these have been identified. With new numerical techniques for its evaluation [16], together with the availability of freely downloadable MATLAB files [12], it is hoped that future workers will incorporate it as a theoretical and computational tool in their investigations of problems in multiply connected domains.

## Acknowledgements

This article surveys some of the ideas presented in a plenary lecture delivered by the author at the 2011 ANZIAM conference, held in Glenelg, South Australia, in January 2011. The author acknowledges support from an EPSRC Advanced Research Fellowship. He also acknowledges the Australian Mathematical Sciences Institute for providing financial support for his 2011 AMSI Lecturer tour in February 2011.

## References

[1] H. F. Baker, *Abelian functions: Abel's theorem and the allied theory of theta functions* (Cambridge University Press, Cambridge, 1897).

[2] S. Bergman, *The kernel function and conformal mapping*, Volume 5 of *Mathematical Surveys* (American Mathematical Society, Providence, RI, 1950).

[3] W. Burnside, "On functions determined from their discontinuities and a certain form of boundary condition", *Proc. Lond. Math. Soc.* **22** (1890) 346–358; doi:10.1112/plms/s1-22.1.346.

[4] D. G. Crowdy, "Analytical formulae for source and sink flows in multiply connected domains", *Theor. Comput. Fluid Dyn.*, to appear; doi:10.1007/s00162-012-0258-x.

[5] D. G. Crowdy, "The Schwarz–Christoffel mapping to bounded multiply connected polygonal domains", *Proc. R. Soc. A* **461** (2005) 2653–2678; doi:10.1098/rspa.2005.1480.

[6] D. G. Crowdy, "Schwarz–Christoffel mappings to unbounded multiply connected polygonal regions", *Math. Proc. Cambridge Philos. Soc.* **142** (2007) 319–339; doi:10.1017/S0305004106009832.

[7] D. G. Crowdy, “Multiple steady bubbles in a Hele-Shaw cell”, *Proc. R. Soc. A.* **465** (2009) 421–435; doi:10.1098/rspa.2008.0252.

[8] D. G. Crowdy, “A new calculus for two-dimensional vortex dynamics”, *Theor. Comput. Fluid Dyn.* **24** (2010) 9–24; doi:10.1007/s00162-009-0098-5.

[9] D. G. Crowdy, “The Schottky–Klein prime function on the Schottky double of planar domains”, *Comput. Methods Funct. Theory* **10** (2010) 501–517.

[10] D. G. Crowdy, “Frictional slip lengths for unidirectional superhydrophobic grooved surfaces”, *Phys. Fluids* **23** (2011) 072001; doi:10.1063/1.3605575.

[11] D. G. Crowdy, A. S. Fokas and C. C. Green, “Conformal mappings to multiply connected polycircular arc domains”, *Comput. Methods Funct. Theory* **11** (2011) 685–706.

[12] D. G. Crowdy and C. C. Green, “The Schottky–Klein prime function”, http://www2.imperial.ac.uk/~dgcrowdy/SKPrime.

[13] D. G. Crowdy and C. C. Green, “Analytical solutions for von Kármán streets of hollow vortices”, *Phys. Fluids* **23** (2011) 126602; doi:10.1063/1.3665102.

[14] D. G. Crowdy and J. S. Marshall, “Analytical formulae for the Kirchhoff–Routh path function in multiply connected domains”, *Proc. R. Soc. A* **461** (2005) 2477–2501; doi:10.1098/rspa.2005.1492.

[15] D. G. Crowdy and J. S. Marshall, “Conformal mappings between canonical multiply connected domains”, *Comput. Methods Funct. Theory* **6** (2006) 59–76.

[16] D. G. Crowdy and J. S. Marshall, “Computing the Schottky–Klein prime function on the Schottky double of planar domains”, *Comput. Methods Funct. Theory* **7** (2007) 293–308.

[17] T. K. DeLillo, “Schwarz–Christoffel mapping of bounded, multiply connected domains”, *Comput. Methods Funct. Theory* **6** (2006) 275–300.

[18] T. K. DeLillo, T. A. Driscoll, A. R. Elcrat and J. A. Pfaltzgraff, “Computation of multiply connected Schwarz–Christoffel maps for exterior domains”, *Comput. Methods Funct. Theory* **6** (2006) 301–315.

[19] T. K. DeLillo, A. R. Elcrat and J. A. Pfaltzgraff, “Schwarz–Christoffel mapping of multiply connected domains”, *J. Anal. Math.* **94** (2004) 17–47; doi:10.1007/BF02789040.

[20] T. A. Driscoll and L. N. Trefethen, *Schwarz–Christoffel mapping* (Cambridge University Press, Cambridge, 2002).

[21] J. D. Fay, *Theta functions on Riemann surfaces*, Volume 352 of *Lecture Notes in Mathematics* (Springer, New York, 1973).

[22] G. M. Goluzin, *Geometric theory of functions of a complex variable*, Volume 26 of *Translations of Mathematical Monographs* (American Mathematical Society, Providence, RI, 1969).

[23] B. Gustafsson, “Quadrature identities and the Schottky double”, *Acta Appl. Math.* **1** (1983) 209–240; doi:10.1007/BF00046600.

[24] D. A. Hejhal, *Theta functions, kernel functions, and Abelian integrals*, Volume 129 of *Memoirs of the American Mathematical Society* (American Mathematical Society, Providence, RI, 1972).

[25] F. Klein, “Zur Theorie der Abel’schen Functionen”, *Math. Ann.* **36** (1890) 1–83; doi:10.1007/BF01199432.

[26] L. M. Milne-Thomson, *Theoretical hydrodynamics*, 5th edn (Dover, New York, 2011).

[27] Z. Nehari, *Conformal mapping* (Dover, New York, 1952).

[28] J. R. Philip, “Flows satisfying mixed no-slip and no-shear conditions”, *Z. Angew. Math. Phys. (ZAMP)* **23** (1972) 353–372; doi:10.1007/BF01595477.

[29] D. Quéré, “Wetting and roughness”, *Ann. Rev. Mat. Res.* **38** (2008) 71–99; doi:10.1146/annurev.matsci.38.060407.132434.

[30] P. G. Saffman, *Vortex dynamics* (Cambridge University Press, Cambridge, 1992).

[31] M. Schiffer, “Recent advances in the theory of conformal mapping”, appendix to: R. Courant, *Dirichlet’s principle, conformal mapping, and minimal surfaces* (Interscience Publishers, New York, 1950).

[32] F. Schottky, “Über eine specielle Function welche bei einer bestimmten linearen Transformation ihres Arguments unverändert bleibt”, *J. reine angew. Math.* **101** (1887) 227–272.

[33] L. I. Sedov, *Two-dimensional problems in hydrodynamics and aerodynamics* (Wiley, London, 1965).

[34] G. I. Taylor and P. G. Saffman, “A note on the motion of bubbles in a Hele-Shaw cell and porous medium”, *Q. J. Mech. Appl. Math.* **12** (1959) 265–279; doi:10.1093/qjmam/12.3.265.

[35] G. Valiron, *Cours d’analyse mathématique: Théorie des fonctions*, 3rd edn (Masson et Cie, Paris, 1966).

[36] E. T. Whittaker and G. N. Watson, *A course of modern analysis* (Cambridge University Press, Cambridge, 1927).